

# A NEW DUAL-COAXIAL-TEM CELL

Hans A. Wolfspenger, Heiko Strehlow, Adolf J. Schwab  
 Institute for Electric Energy Systems and High Voltage Technologie  
 University of Karlsruhe, Kaiserstraße 12, 76128 Karlsruhe, Germany.  
 email: wolfspenger@ieh.etec.uni-karlsruhe.de

**Abstract:** Previously, different configurations of TEM cells, chambers and transmission-line holders were used to determine the intrinsic Shielding Effectiveness (SE) of materials e.g. conductive plastics. In this contribution, a new *Dual-Coaxial-TEM Cell* is presented which allows to measure the SE of materials, determine the influence of apertures and test analytical and numerical computation methods. The mechanical and electrical structure is described and the calculation of the electromagnetic coupling is verified by the results of measurements. In addition to the worst-case examination of structures (the electric field is perpendicular to the surface of the test-sample), the Dual-Coaxial-TEM Cell provides a wide frequency range and high dynamic.

## INTRODUCTION

Conventional *Dual-TEM Cells* consist of two single TEM cells, coupled by a common aperture, where the test sample can be inserted. In contrast to other designs (e.g. transmission line holder), the electric field is perpendicular and the magnetic field is parallel to the test sample, both in a well defined way [1]-[4]. The frequency range is limited by the cut-off frequency of the lowest mode  $TE_{10}$ . A dynamic range of 100 dB and more at high frequencies can be realized.

Until now, dual cells had a rectangular cross section. According to Kaden's calculation of electromagnetic coupling between coaxial transmission-lines [5],[6], a new *Dual-Coaxial-TEM Cell* was developed, Fig. 1 and 2. It consists of two tapered coaxial lines of circular cross section with a common window,  $5 \times 6 \text{ cm}^2$ . The test-sample – a simple rectangular plate – is placed in between, thightened with screws, which provides a good contact.

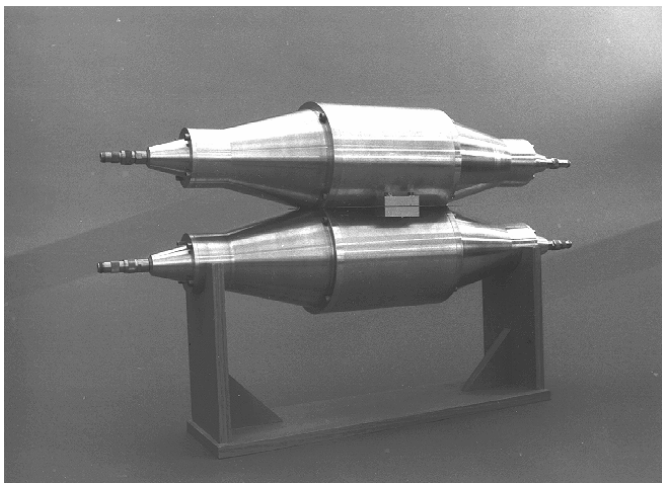


Fig.1: Dual-Coaxial-TEM Cell

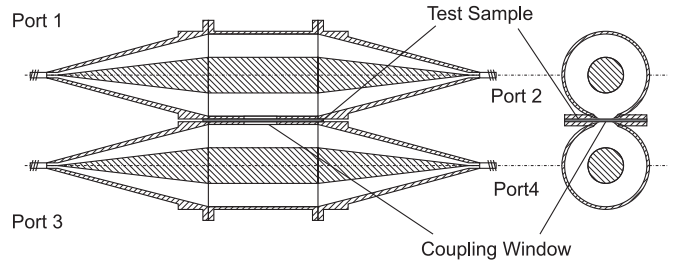


Fig.2: Longitudinal- and cross-section of the Dual-Coaxial-TEM Cell

For standard SE measurements [4, pp. 3.14-3.17], the dual cell is connected to a signal source (e.g. of a spectrum analyzer) at port 1 while port 2 is terminated with a  $50 \Omega$  load. For a higher dynamic range it might be necessary to use an amplifier. Thus, a TEM wave with radial electric and azimuthal magnetic field components is generated in the transmitting cell. Electric and magnetic coupling between the cells through the common window excites a TEM wave in the receiving cell, which is absorbed by the impedance of a test receiver connected at port 4 and a termination load at port 3. The difference of voltage levels measured with and without test-sample between the cells is the Shielding Effectiveness SE:

$$SE \text{ [dB]} = u_{\text{without sample}} - u_{\text{with sample}} \quad (1)$$

Instead of measuring the SE with the receiver at the opposite end of the dual cell, as it is described in an NBS standard, the SE can be measured at the near end.

For all SE measurements with symmetric dual cells it is important to know whether they are made using the output near to or far from the generator. The difference of two options is described in the last section of this contribution.

## PROPERTIES OF THE DUAL-COAXIAL-TEM CELL

During the design process of the Dual-Coaxial-TEM Cell, two points were considered to be most important: Avoiding reflections and suppressing higher order modes [7],[8]. Besides choosing the right geometry to provide a constant characteristic impedance there are no dielectric supports inside. This is possible because the inner conductors, consisting of steel and aluminum, are weight-optimized and so their slack is reduced. Parallel slots in the inner conductors are suppressing tangential eddy currents of higher order H-modes. For the same purpose the outer conductor's cone angle in the feeding section is only  $30^\circ$ , the inner conductor's is  $13.5^\circ$ .

A TDR measurement of one single cell, seperated from the other by a massive aluminum plate, shows the quality of impedance matching, Fig. 3:

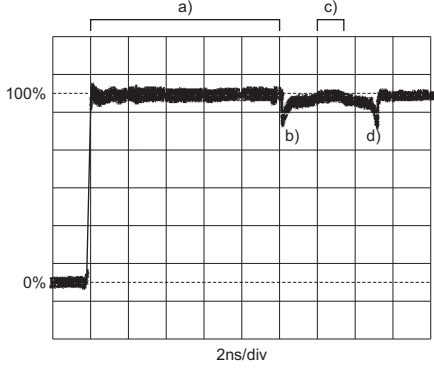


**Fig 3:** TDR measurement of one single cell. a): Feed line, b) and d): Connectors. c): Area of the coupling window.

Only at the tips of the inner conductor where its diameter is only 3mm, there is a small mismatch, having its roots in the tolerance of the connection to the N-jack. The reflection factor at this section is about 2% which corresponds to a characteristic impedance of 48  $\Omega$ . However, frequency domain measurements show zeroes of the total reflection factor  $S_{11}$  every 200 MHz (Fig. 4), equal to a wavelength of 1.5 m in air which is twice the length of one cell.

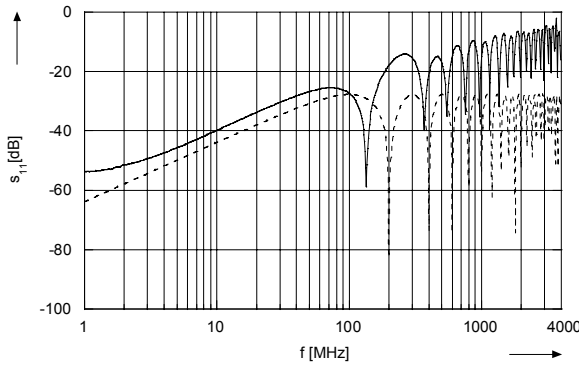


**Fig. 4:** Total reflection coefficient  $S_{11}$  of one Coaxial-TEM cell, measured  $\text{---}$  and calculated  $\text{- - -}$ .

This behaviour has its roots in the reflections caused by the tips, interfering in a destructive way when the phase shift between the reflected waves is a multiple of  $2\pi$ . It can be approximately calculated with a simple model of concatenated scattering matrices [9], [10]. The regular conventions of waves of a two-port are shown in Fig. 5 a).

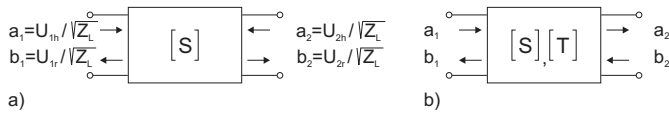


**Fig. 5:** a) Regular conventions of waves of a two-port, b) conventions for serial connection of two-ports.

To combine several scattering matrices, the semantics of the wave conventions have to be changed, while the S-matrix itself stays the same, Fig. 5 b). One TEM cell can be considered as a series of three two-ports; an irregularity, a transmission line and an irregularity again, Fig. 6.

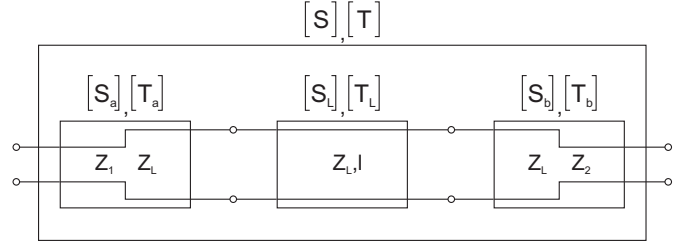


**Fig. 6:** Three scattering matrices modelling a single cell.

The scattering matrices are given by:

$$[S_a] = \begin{bmatrix} \frac{Z_L - Z_1}{Z_L + Z_1} & \sqrt{1 - \left(\frac{Z_L - Z_1}{Z_L + Z_1}\right)^2} \\ \sqrt{1 - \left(\frac{Z_L - Z_1}{Z_L + Z_1}\right)^2} & -\frac{Z_L - Z_1}{Z_L + Z_1} \end{bmatrix} \quad (2)$$

$$[S_L] = \begin{bmatrix} 0 & e^{(-\gamma l)} \\ e^{(-\gamma l)} & 0 \end{bmatrix} \quad (3)$$

$$[S_b] = \begin{bmatrix} \frac{Z_2 - Z_L}{Z_2 + Z_L} & \sqrt{1 - \left(\frac{Z_2 - Z_L}{Z_2 + Z_L}\right)^2} \\ \sqrt{1 - \left(\frac{Z_2 - Z_L}{Z_2 + Z_L}\right)^2} & -\frac{Z_2 - Z_L}{Z_2 + Z_L} \end{bmatrix} \quad (4)$$

Obtaining the scattering matrix  $[S]$  of the whole series requires conversion of the single matrices  $[S_a]$ ,  $[S_L]$  and  $[S_b]$  into transmission matrices  $[T_a]$ ,  $[T_L]$  and  $[T_b]$ .

The conversion matrix is

$$[T_x] = \begin{bmatrix} S_{x12} - S_{x11}S_{x21}^{-1}S_{x22} & S_{x11}S_{x21}^{-1} \\ -S_{x21}^{-1}S_{x22} & S_{x21}^{-1} \end{bmatrix} \quad (5)$$

The total transmission matrix  $[T]$  is obtained from

$$[T] = [T_a] \cdot [T_L] \cdot [T_b] \quad (6)$$

$[T]$  can be re-converted to  $[S]$  by

$$[S] = \begin{bmatrix} T_{12}T_{22}^{-1} & T_{11} - T_{12}T_{22}^{-1}T_{21} \\ T_{22}^{-1} & -T_{22}^{-1}T_{21} \end{bmatrix} \quad (7)$$

If this procedure is done with the single scattering matrices (2), (3), (4) for the scattering parameters of the total scattering matrix  $[S]$  in the case of  $Z_1=Z_2=Z$  one obtains:

$$S_{11} = S_{22} = \frac{Z^3 + Z^2Z_L - ZZ_L^2 - Z_L^3}{(Z + Z_L)\left((Z + Z_L)^2 e^{2\gamma l} - (Z - Z_L)^2\right)} + \frac{Z^2 - Z_L^2}{(Z - Z_L)^2 e^{-2\gamma l} - (Z + Z_L)^2} \quad (8)$$

$$S_{21} = S_{12} = \frac{4ZZ_L}{-(Z - Z_L)^2 e^{-\gamma l} + (Z + Z_L)^2 e^{\gamma l}} \quad (9)$$

$S_{11}$  is also shown in Fig. 5. Although the zeros are not exactly met (in reality the reflexions are not caused by only two irregularities without any length), the effect of the multiple reflexions can be understood.

The resulting values of  $S_{21}$  are in a range of 0 - 0.01 dB and therefore not shown together with the measurement result in Fig. 7, below.

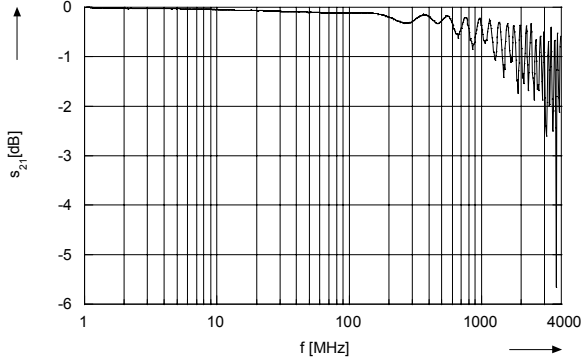


**Fig. 7:** Measured transmission coefficient of one Coaxial-TEM cell. Calculated values in a range of 0 - 0.01 dB, not shown.

The dynamic range was determined by measurements without any test sample and with a massive brass plate between the two cells. For frequencies below 10 MHz it is limited by the shielding effectiveness of the outer conductors' aluminum and the brass, for higher frequency by the receiver's noise. The dynamic range, shown in Fig. 8, can be improved by using a more powerful amplifier.

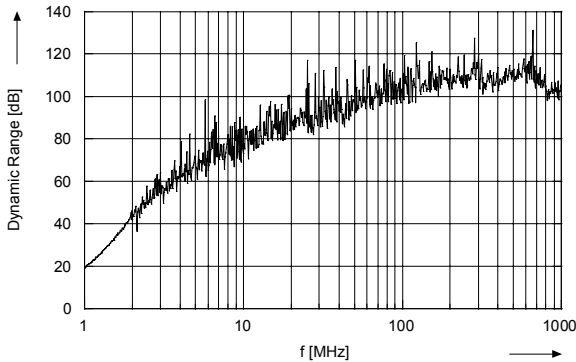


**Fig. 8:** Dynamic range of the Dual-Coaxial-TEM cell, determined using an amplifier with 25 dBm output power.

### MEASUREMENT OF PERFORATED STRUCTURES

It is possible to describe the magnetic and the electric coupling between transmission lines – a Dual-TEM cell can be considered as two lines – by a coupling capacitance and a coupling inductance [5],[6], shown in the circuit model, Fig. 9:

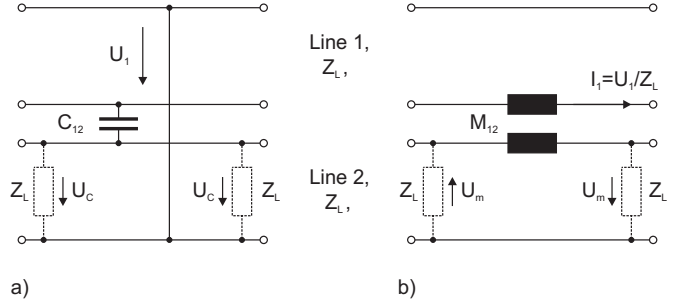


**Fig. 9:** Circuit model for a) electric coupling and b) magnetic coupling between two transmission lines.

Excitation of transmission line 1 influences in transmission line 2 the voltage

$$U_c = \frac{\frac{1}{2} j\omega C_{12} Z_L U_1}{\frac{1}{2} j\omega C_{12} Z_L U_1 + 1} \approx \frac{1}{2} j\omega C_{12} Z_L U_1, \quad (10)$$

$$\frac{1}{2} \omega C_{12} Z_L U_1 \ll 1$$

by autocapacitive coupling and induces the voltage

$$U_m = \frac{1}{2} j\omega M_{12} \frac{U_1}{Z_L} \quad (11)$$

by autoinductive coupling. Using the circuit model, for the voltages  $U_n$  and  $U_f$  measured at the near and the far end of transmission line 2 one obtains:

$$U_n = U_c + U_m \quad (12)$$

$$U_f = U_c - U_m \quad (13)$$

This is important, because although the test set-up is absolutely symmetric, it is not equal if the measurement is done near or the far to the generator. Using (12) and (13) it is possible to obtain the electric and the magnetic shielding effectiveness separately, which is not taken in account in standard SE measurements.

However, the most important question is the magnitude of coupling. According to Kaden the coupling inductance of a circular hole between two coaxial lines is

$$M_{12} = \frac{\mu_0 r_0^3}{3\pi^2} \frac{1}{r_{a1} r_{a2}} \quad (14)$$

and the coupling capacity

$$C_{12} = \frac{r_0^3 C'_1 C'_2}{6\pi^2 \epsilon_0} \frac{1}{r_{a1} r_{a2}} \quad (15)$$

$C'_1$  and  $C'_2$  are the capacitances per unit length of the lines,  $r_{a1}$  and  $r_{a2}$  are the outer conductors' radii and  $r_0$  is the radius of the common circular aperture. Using (10) - (13) the transmission factor for the coupled dual cell can be calculated. It is compared to the measurement results in Fig. 10:

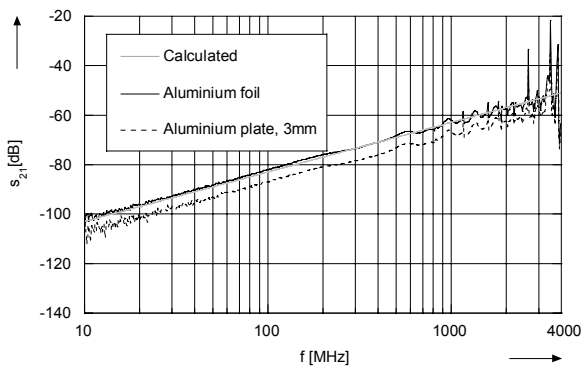


**Fig. 10:** Calculated and measured transmission factor in dB (near the generator). Inserted sample with a 20 mm circular aperture.

Measurement and theory are very close, until 1000 MHz plus, when resonances are influencing the result. The measurement was done with a perforated aluminum foil to compare it with the calculation for an infinitesimal thin wall between the cells. Using a 3 mm thick aluminum plate, the attenuation increases about 5 dB.

Finally, measuring the transmission between the dual cells without any sample a reference is obtained. Using (1) this allows to present measurement results as insertion loss, Fig. 11:

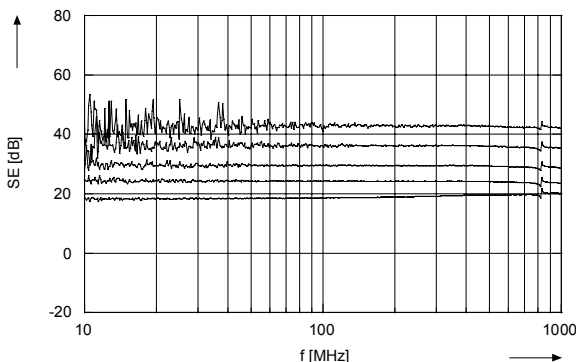


**Fig. 11** Insertion loss measurement of samples with circular holes of different diameters. Downwards: 13 mm, 16 mm, 20 mm, 24 mm, 30 mm.

These measurements were made using a network analyzer. Using an amplifier, the noise at lower frequency can be eliminated.

### CONCLUSIONS

A new kind of Dual-TEM Cell with circular cross section offers worst case measurements of intrinsic SE and the determination of apertures' influence. Besides a large frequency range and high dynamic there is the advantage of simple rectangular test samples, which can be easily bonded. The measured properties of the dual cell can be verified by calculations. Determination of electromagnetic coupling through circular holes is easy and precise, the results agree with analytical calculations very well.

### REFERENCES

- [1] P. F. Wilson e.a., „Techniques fo Measuring the Electromagnetic Shielding Effectiveness of Materials: Part I:– Far-Field Source Simulation“, IEEE Transactions on EMC, Vol. 30, No. 3, 1988.
- [2] P. F. Wilson e.a., „Techniques fo Measuring the Electromagnetic Shielding Effectiveness of Materials: Part II:– Near-Field Source Simulation“, IEEE Transactions on EMC, Vol. 30, No. 3, 1988.
- [3] A. J. Schwab „Elektromagnetische Verträglichkeit“, 3. Auflage, Springer-Verlag, pp. 377 - 385, 1994.
- [4] D. R. J. White and M. Mardiguan, „Electromagnetic Shielding“, Handbook Series on Electromagnetic Interference an Compatibility, Vol. 3., 1988
- [5] H. Kaden, „Wirbelströme und Schirmung in der Nachrichtentechnik“, Springer-Verlag, 1959.
- [6] H. Kaden, „Loch- und Schlitzkopplungen zwischen koaxialen Leitungssystemen“, Zeitschrift für angewandte Physik, III. Band, Heft 2, pp. 44 - 52, 1951.
- [7] M. Koch, H. Garbe, „Geometrieabhängige Modenanlyse einer kompletten TEM-Zelle“, EMV '96 Karlsruhe, 5<sup>th</sup> International Exhibition and Congress, pp. 325 - 332, 1996.
- [8] M. Koch, H. Garbe, „Investigation of Field Distorsion in a TEM Waveguide“, 11<sup>th</sup> International Zürich Symposium and Technical Exhibition on Electromagnetic Compatibility, pp. 595 - 598, 1995.
- [9] O. Zinke, H. Brunswig, „Hochfrequenztechnik 1“, 5. Auflage, Springer-Verlag, 1995
- [10] H. Meinke, F. W. Gundlach, „Taschenbuch der Hochfrequenztechnik“, 5. Auflage, Springer-Verlag, 1992